J. Phys. B: At. Mol. Opt. Phys. 27 (1994) L663–L669. Printed in the UK

LETTER TO THE EDITOR

Soft x-ray spectrum of a laser-produced gallium plasma

T Döhring†§, J Stiehler‡, N Böwering† and U Heinzmann†

† Fakultät für Physik, Universität Bielefeld, D-33501 Bielefeld, Germany

‡ Fakultät für Chemie, Universität Bielefeld, D-33501 Bielefeld, Germany

Received 25 August 1994

Abstract. We report here on new spectroscopic measurements of transitions in highly ionized gallium. Employing a Nd:YAG laser and a grazing incidence monochromator with toroidal grating, the soft x-ray spectrum of a laser-produced gallium plasma was observed in the wavelength region between 2 and 13.5 nm. Using in addition the results of Hartree–Fock calculations, the dominant transition arrays of the ionization stages Ga VII to Ga XIV have been classified. The main lines are ascribed to the $3p^63d^{n-1}4f$–$3p^63d^n$ transitions ($n = 1$–7); furthermore, 5f–3d, 6f–3d, 3d–3p and 4p–3d emission lines were identified.

Laser-produced plasmas emit intense radiation in the soft x-ray region and therefore they are often employed as light sources. For several applications such laboratory light sources are an interesting supplement and a low-cost alternative to synchrotron radiation facilities. In addition, the spectra of laser-induced plasmas provide detailed information on the transitions and electronic structure of highly ionized atoms, as discussed in several recent review articles (Fawcett 1984, Martinson 1989, O'Sullivan 1992). While this knowledge is complete or nearly complete for the light elements up to iron, areas of ionization stages with no or almost no information exist for ions of the heavier elements. In particular, in the case of gallium, very little or no knowledge is available for the ionization stages from Ga VI to Ga LXX, as a recent compilation presented by Martinson (1989) shows. To partially fill in this gap we report here on the spectrum in the soft x-ray region for a laser-produced gallium plasma and its analysis covering transitions of the ionization stages from Ga VII to Ga XIV. These ionization levels, which are characterized in the ground state by complete electron shells up to the 3p subshell and a partially filled 3d subshell, are reached by successive ejection of the 3d electrons. Our data build on previous results for a few $n = 4$–3 transitions of highly ionized gallium reported by Fawcett and Hayes (1975).

We used the pulsed 1064 nm radiation of a table-top Nd:YAG laser system (up to 1000 mJ pulse energy, 8 ns pulse duration, 10 Hz repetition rate) to produce power densities of up to 10^{13} W cm^{-2} on the target surface. In order to prevent the formation of craters on the surface of the gallium target it was molten in a resistively heated furnace at temperatures of about 500 K. The furnace was covered by a cylindrical lid in thermal contact, leaving holes only for the laser entrance and the radiation emitted into a small angular cone towards the monochromator. This way, the escape of droplets and vaporized material was suppressed and a partial recycling of the escaping gallium material could be achieved. Because of the occurence of a destructive alloying process, any direct contact of gallium with aluminium parts had to be prevented. For laser intensities up to 500 mJ at a repetition rate of 10 Hz the

§ Present address: GSF-Forschungszentrum, D-85758 Oberschleißheim, Germany.

0953-4075/94/190663+07$19.50

light emission from the liquid target configuration is stable to within 4% over some 10 000 shots. The shot-to-shot x-ray fluctuations are dominated by the laser output variations. At higher laser intensities the creation of droplets increases and a long-term measurement becomes more difficult. The technical aspects of the liquid source for XUV application will be discussed elsewhere.

The emitted soft x-ray spectra were observed at an angle of 80° to the incident laser radiation by means of a grazing incidence monochromator, which is similar in design to the instrument of Dietz *et al* (1985), but with entrance and exit arm lengths of 1.58 nm and 2.08 m, respectively. A gold-coated toroidal grating of 1000 lines/mm was employed at a deflection angle of 170° to obtain focussing and dispersion of the emitted XUV radiation using only one optical element with high transmission and low aberrations. The microplasma itself forms the entrance aperture and the exit slit is fixed. The monochromator covers the spectral range from nominally 2 to 12 nm (maximum range: 1.5–15 nm) and is constructed for high transmission (3 mrad×20 mrad acceptance angle) at moderate wavelength resolution (typically $\lambda/\Delta\lambda = 50$–$100$ at a width of 1 mm for the exit slit). The wavelength calibration of the monochromator was carried out by plasma spectroscopy on different solid low-Z targets, where the line spectra could be separated with our resolution. By use of known transitions of aluminium, carbon, nitrogen and boron ions (Bashkin and Stoner 1975) a calibration was achieved to an accuracy within the experimental uncertainty of ±0.04 nm. Behind the monochromator exit slit absolute photon intensities were measured with GaAsP photodiodes (Hamamatsu G1127-02). This type of detector has been calibrated at the PTB in Berlin (Krumrey *et al* 1988).

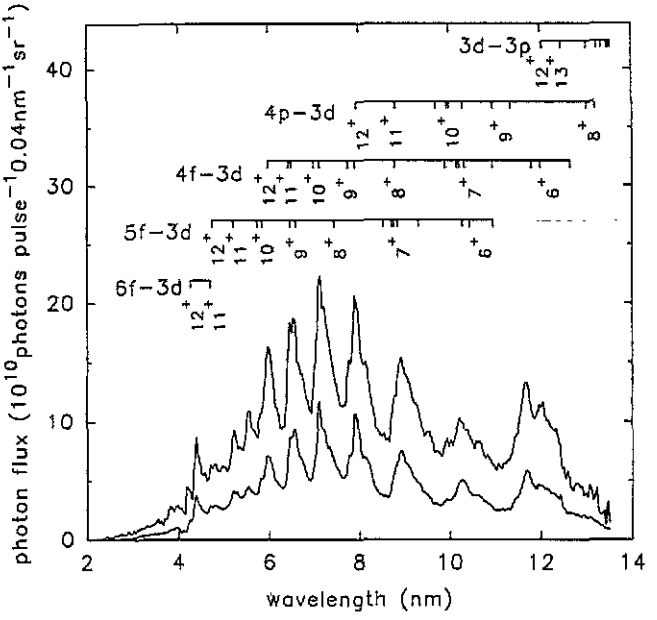

Figure 1. Soft x-ray spectra of a gallium plasma obtained at laser pulse energies of 500 mJ (top) and 300 mJ (bottom). The calculated positions of line groups classified for different ionization stages and different transitions are marked in the upper part of the figure.

In figure 1 the observed spectrum for laser pulse energies of 300 mJ and 500 mJ is plotted. The spectrum is divided into seven fairly regular structures between 6 and 12 nm

indicating that the dominant transitions for each ionization level of gallium corresponding to a successively increasing number of 3d electrons do not overlap. The intensity scale reflects the detected absolute number of photons at 80° observation angle, corrected for the collection angle and the transmission of the monochromator and the wavelength-dependent transmission of an 0.45 μm thick capton foil, which was inserted in the entrance arm of the monochromator to protect the grating. The transmission of the monochromator without capton foil has been calculated to be nearly wavelength independent between 2 and 12 nm and has been measured to be 2.5% $\pm$ 0.5% at 4 nm. The uncertainty in the scale of the absolute value of the detected photon flux is about 15%. The measured x-ray signal is integrated over the temporal pulse duration and the spatial plasma extension. Each data point is the mean value of 10 laser pulses; for a complete spectrum typically 20 000 pulses were accumulated.

Assuming local thermal equilibrium (LTE) as a coarse approximation, the mean electron temperatures can be determined from the increase of the intensity in the short wavelength part of the spectrum below 4 nm, as described previously for other laser targets (Böwering *et al* 1991). Within the LTE model the mean electron temperatures of the gallium plasmas were found to lie between 30 and 50 eV in the plotted cases.

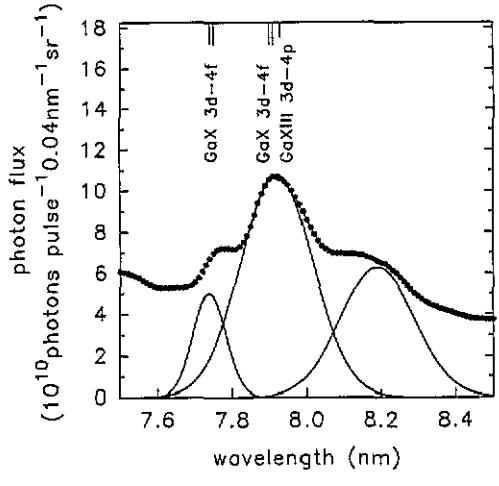

Figure 2. Expanded view of a section of the gallium spectrum at 300 mJ laser pulse energy. The fitted Gauss profiles and the calculated line positions are plotted in addition to indicate the positions of the line groups.

In figure 2 a group of lines at around 8 nm is shown in detail. The spectrum has been fitted by Gaussian line profiles. When subtracting the profiles of the high intensity peaks, the positions of the lower intensity peaks in shoulders can also be determined. The fitted line profiles for gallium are much broader than for low-Z elements at the same wavelength. At a wavelength of 8 nm the resolution of the monochromator measured using a lithium-fluoride plasma is about $\lambda/\Delta\lambda = 100$ for a 1 mm wide exit slit. The broadening indicates a superposition of different substates of gallium ions.

The lines of the gallium spectrum (figure 1) split up in clusters of different substate transitions (see below), reflecting the fine structure of the ions. These substates are superimposed and cannot be separated with our resolution. Furthermore, in some cases it is difficult to define the exact position of the line centre. Nevetheless, it was possible to

Table 1. Table of experimentally observed positions of line groups, corresponding photon energies, peak heights and peak widths for the gallium plasma. Lines overlapping within the experimental precision with transitions also observed by Fawcett and Hayes (1975) are marked by an asterisk.

Wavelength (nm) (±0.04 nm)	Corresponding photon energy (eV)	Peak height (10^{10} photons pulse^{-1} 0.04 nm^{-1} sr^{-1})	$\lambda/\Delta\lambda_{FWHM}$
12.03*	103.0	4.0	50
11.69	106.0	5.9	33
11.37	109.0	2.6	50
10.83	114.4	2.9	35
10.61	116.8	1.8	50
10.28	120.6	5.0	22
9.89	125.3	2.6	40
9.68	128.0	2.0	50
9.53	130.0	2.1	50
9.31	133.1	4.6	30
8.92	138.9	7.5	30
8.73	142.0	2.8	65
8.19	151.4	6.3	35
7.92	156.5	10.8	35
7.74	160.2	5.0	75
7.31	169.5	6.9	85
7.23	171.5	6.9	75
7.10	174.5	11.7	50
6.97	177.8	5.2	70
6.75	183.7	5.3	40
6.55	189.3	9.3	30
6.43*	192.8	4.2	80
5.97*	207.7	7.1	22
5.78	214.5	3.0	50
5.56*	223.0	4.2	50
5.24*	236.5	3.9	50
4.73	262.0	2.5	35
4.38	283.0	3.5	30
4.23	293.1	1.4	40

deduce more than twenty ionic lines or line group positions and these are listed in table 1. In some spectral regions additional lines could not be separated. For the interpretation of this table the following restrictions have to be considered: as discussed above, it is difficult to define the wavelength position of blended lines. These uncertainties and the wavelength calibration uncertainties lead to the error specified. The intensity values listed in table 1 represent the observed peak heights of the lines at 300 mJ laser pulse energy. These values strongly depend on the plasma conditions and also on the resolution of the monochromator.

To obtain a basis for the identification of the observed lines of highly ionized gallium, the transition energies in the range between 100 eV and 300 eV for different ionization stages were computed using a numerical Hartree–Fock program (Hinze and Stiehler 1992). Transitions to the ground state with the selection rules $\Delta M_L = \pm 1$ and $\Delta M_S = 0$ were considered, as these are the most intense lines in the spectra of isoelectronic ions. To estimate the error due to the electron correlation effect, the calculated transition energies were compared with corresponding spectroscopic data for isoelectronic ions (Shirai *et al* 1990, 1991, Kaufmann *et al* 1989, Moore 1971). The deviation is found to be below 1 eV in nearly all cases, the only exceptions being transitions from the configuration $3p^5 3d^{n+1}$

Table 2. Hartree–Fock calculated transition energies and ionization energies for gallium ions.

Transition energy (eV)	Transition
Ga XV (14^+, Cl sequence)	$I_p = 507.4 \pm 1.0$ eV
93.8 ± 1.0	$3p^5\ ^2P$–$3p^4 3d\ (^3P)\ ^2D$
Ga XIV (13^+, Ar sequence),	$I_p = 471.2 \pm 1.0$ eV
99.5 ± 0.5	$3p^6\ ^1S$–$3p^5 3d\ (^2P)\ ^1P$
Ga XIII (12^+, K sequence),	$I_p = 358.1 \pm 1.0$ eV
95.3 ± 0.3	$3p^6 3d\ ^2D$–$3p^5 3d^2\ (^1G)\ ^2F$
103.0 ± 0.3	$3p^6 3d\ ^2D$–$3p^5 3d^2\ (^3F)\ ^2D$
103.0 ± 0.3	$3p^6 3d\ ^2D$–$3p^5 3d^2\ (^3P)\ ^2P$
156.4 ± 0.2	$3p^6 3d\ ^2D$–$3p^6 4p\ (^1S)\ ^2P$
207.4 ± 0.2	$3p^6 3d\ ^2D$–$3p^6 4f\ (^1S)\ ^2F$
261.4 ± 0.2	$3p^6 3d\ ^2D$–$3p^6 5f\ (^1S)\ ^2F$
290.9 ± 0.2	$3p^6 3d\ ^2D$–$3p^6 6f\ (^1S)\ ^2F$
Ga XII (11^+, Ca sequence),	$I_p = 321.1 \pm 1.0$ eV
91.6 ± 0.5	$3p^6 3d^2\ ^3F$–$3p^5 3d^3\ (^2H)\ ^3G$
91.9 ± 0.5	$3p^6 3d^2\ ^3F$–$3p^5 3d^3\ (^4F)\ ^3F$
140.7 ± 0.3	$3p^6 3d^2\ ^3F$–$3p^6 3d4p\ (^2D)\ ^3D$
141.3 ± 0.3	$3p^6 3d^2\ ^3F$–$3p^6 3d4p\ (^2D)\ ^3F$
191.2 ± 0.3	$3p^6 3d^2\ ^3F$–$3p^6 3d4f\ (^2D)\ ^3F$
192.7 ± 0.3	$3p^6 3d^2\ ^3F$–$3p^6 3d4f\ (^2D)\ ^3G$
237.6 ± 0.3	$3p^6 3d^2\ ^3F$–$3p^6 3d5f\ (^2D)\ ^3F$
238.5 ± 0.3	$3p^6 3d^2\ ^3F$–$3p^6 3d5f\ (^2D)\ ^3G$
263.2 ± 0.3	$3p^6 3d^2\ ^3F$–$3p^6 3d6f\ (^2D)\ ^3F$
263.6 ± 0.3	$3p^6 3d^2\ ^3F$–$3p^6 3d6f\ (^2D)\ ^3G$
Ga XI (10^+, Sc sequence),	$I_p = 283.0 \pm 1.0$ eV
88.4 ± 2.0	$3p^6 3d^3\ ^2H$–$3p^5 3d^4\ (^3D)\ ^4F$
92.1 ± 2.0	$3p^6 3d^3\ ^2H$–$3p^5 3d^4\ (^3G)\ ^4F$
93.0 ± 2.0	$3p^6 3d^3\ ^2H$–$3p^5 3d^4\ (^3H)\ ^4G$
93.8 ± 2.0	$3p^6 3d^3\ ^2H$–$3p^5 3d^4\ (^5G)\ ^4F$
120.5 ± 0.3	$3p^6 3d^3\ ^2H$–$3p^6 3d^2 4p\ (^3F)\ ^2G$
124.2 ± 0.3	$3p^6 3d^3\ ^4F$–$3p^6 3d^2 4p\ (^3F)\ ^4F$
124.9 ± 0.3	$3p^6 3d^3\ ^4F$–$3p^6 3d^2 4p\ (^3F)\ ^4D$
128.1 ± 0.3	$3p^6 3d^3\ ^4F$–$3p^6 3d^2 4p\ (^3P)\ ^2D$
174.3 ± 0.4	$3p^6 3d^3\ ^4F$–$3p^6 3d^2 4f\ (^3F)\ ^4F$
177.7 ± 0.4	$3p^6 3d^3\ ^4F$–$3p^6 3d^2 4f\ (^3P)\ ^4F$
212.5 ± 0.4	$3p^6 3d^3\ ^4F$–$3p^6 3d^2 5f\ (^3F)\ ^4F$
216.2 ± 0.4	$3p^6 3d^3\ ^4F$–$3p^6 3d^2 5f\ (^3P)\ ^4F$
Ga X (9^+, Ti sequence),	$I_p = 246.6 \pm 1.0$ eV
109.3 ± 1.0	$3p^6 3d^4\ ^5D$–$3p^6 3d^3 4p\ (^4F)\ ^5D$
113.3 ± 1.0	$3p^6 3d^4\ ^5D$–$3p^6 3d^3 4p\ (^4P)\ ^5D$
156.7 ± 0.6	$3p^6 3d^4\ ^5D$–$3p^6 3d^3 4f\ (^4F)\ ^5F$
157.0 ± 0.6	$3p^6 3d^4\ ^5D$–$3p^6 3d^3 4f\ (^4F)\ ^5D$
159.9 ± 0.6	$3p^6 3d^4\ ^5D$–$3p^6 3d^3 4f\ (^4P)\ ^5F$
160.3 ± 0.6	$3p^6 3d^4\ ^5D$–$3p^6 3d^3 4f\ (^4P)\ ^5D$
188.2 ± 0.6	$3p^6 3d^4\ ^5D$–$3p^6 3d^3 5f\ (^4F)\ ^5F$
191.9 ± 0.6	$3p^6 3d^4\ ^5D$–$3p^6 3d^3 5f\ (^4P)\ ^5F$
Ga IX (8^+, V sequence),	$I_p = 214.2 \pm 1.0$ eV
94.1 ± 0.3	$3p^6 3d^5\ ^4D$–$3p^6 3d^4 4p\ (^5D)\ ^4D$
95.4 ± 0.3	$3p^6 3d^5\ ^6S$–$3p^6 3d^4 4p\ (^5D)\ ^6P$
141.1 ± 0.6	$3p^6 3d^5\ ^6S$–$3p^6 3d^4 4f\ (^5D)\ ^6P$
166.5 ± 0.6	$3p^6 3d^5\ ^6S$–$3p^6 3d^4 5f\ (^5D)\ ^6P$
Ga VIII (7^+, Cr sequence),	$I_p = 171.7 \pm 1.0$ eV
113.3 ± 0.6	$3p^6 3d^6\ ^5D$–$3p^6 3d^5 4f\ (^6S)\ ^5F$
120.0 ± 0.6	$3p^6 3d^6\ ^5D$–$3p^6 3d^5 4f\ (^4G)\ ^5F$

Table 2. (continued)

Transition energy (eV)	Transition
121.4 ± 0.6	$3p^63d^6\ ^5D$–$3p^63d^54f\ (^4P)\ ^5F$
122.1 ± 0.6	$3p^63d^6\ ^5D$–$3p^63d^54f\ (^4D)\ ^5F$
125.3 ± 0.6	$3p^63d^6\ ^5D$–$3p^63d^54f\ (^4F)\ ^5F$
133.1 ± 0.6	$3p^63d^6\ ^5D$–$3p^63d^55f\ (^6S)\ ^5F$
140.1 ± 0.6	$3p^63d^6\ ^5D$–$3p^63d^55f\ (^4G)\ ^5F$
141.4 ± 0.6	$3p^63d^6\ ^5D$–$3p^63d^55f\ (^4P)\ ^5F$
142.1 ± 0.6	$3p^63d^6\ ^5D$–$3p^63d^55f\ (^4D)\ ^5F$
145.3 ± 0.6	$3p^63d^6\ ^5D$–$3p^63d^55f\ (^4F)\ ^5F$
Ga VII (6^+, Mn sequence), $I_p = 143.3 \pm 1.0$ eV	
98.0 ± 0.6	$3p^63d^7\ ^4F$–$3p^63d^64f\ (^5D)\ ^4G$
103.5 ± 0.6	$3p^63d^7\ ^4F$–$3p^63d^64f\ (^3G)\ ^4G$
105.1 ± 0.6	$3p^63d^7\ ^4F$–$3p^63d^64f\ (^3D)\ ^4F$
105.2 ± 0.6	$3p^63d^7\ ^4F$–$3p^63d^64f\ (^3D)\ ^4G$
113.1 ± 0.6	$3p^63d^7\ ^4F$–$3p^63d^65f\ (^5D)\ ^4G$
118.8 ± 0.6	$3p^63d^7\ ^4F$–$3p^63d^65f\ (^3G)\ ^4G$
120.5 ± 0.6	$3p^63d^7\ ^4F$–$3p^63d^65f\ (^3D)\ ^4G$

to the ground state. Spin–orbit interactions would lead to an energy correction within the stated uncertainty of the data and were not taken into account. The computed transition energies and also the ionization potentials of the various gallium ions considered are listed in table 2.

In figure 1 we marked the position of calculated line groups belonging to the same transition type. Comparing the observed spectrum and the calculated line positions, the following qualitative aspects can be deduced for the observed gallium spectra.

(i) In the wavelength region between 4 nm and 12 nm the spectrum is dominated by transitions of highly charged positive ions of gallium, i.e. the argon-like ions (Ga XIV) through the manganese-like (Ga VII) with ground state configurations $3p^63d^n$.

(ii) Considering the intensity distributions in the known isoelectronic spectra, the 4p–3d, 4f–3d and 3d–3p transitions are expected to form the most intense lines.

(iii) The dominant structure of the spectrum is caused by $3p^63d^{n-1}4f$–$3p^63d^n$ transitions of ions up to Ga XIII. Between transitions of successive ionization levels nearly constant photon energy separations are found. Some of the less intense 5f–3d and 6f–3d transitions can also be identified, in particular in the short wavelength part of the spectrum.

(iv) Similarly, the 4p–3d transitions form a group of lines with constant energy separations for different ionization stages. Due to the resolution in our experiment the 4p–3d lines overlap with 4f–3d lines of other ions. Therefore we are unable to estimate relative intensities for the different transitions.

(v) The 3d–3p transitions of the potassium-like Ga XIII can be found at around 12 nm (Fawcett and Hayes 1975, Kaufmann *et al* 1989). For neighbouring lower and higher ionization stages these lines are shifted towards longer wavelength. Because this region is near the long-wavelength limit of our monochromator these lines could not be resolved.

An exact identification of individual lines is complicated by the large number of LS states which arise out of configurations with several electrons in the 3d shell. In this case the transition energies are spread over a range of up to 10 eV and not all individual lines can be resolved with the present apparatus. Due to the lack of spectral data for isoelectronic sequences it is difficult to estimate the intensity distribution within a line group.

For more detailed investigations, a higher wavelength resolution and the preparation of

individual ionic states is needed. Furthermore, the calculation of transition probabilities, not yet implemented in our HF program, would be useful for the identification of individual lines.

In summary, the spectrum of a laser-induced plasma of a liquid gallium target was observed in the soft x-ray range. It is dominated by the $3p^6 3d^{n-1} 4f$–$3p^6 3d^n$ transitions of Ga XIII to Ga VII ($n = 1$–7) which form a series of line groups in the wavelength region from 6 to 12 nm. Liquid gallium is a new promising target for the application of laser-produced plasmas as x-ray sources.

Assistance during target preparation by R Irrgang and M Pröpper and helpful discussions with J Hinze are gratefully acknowledged. This work was supported by MWF NRW and BMFT (13N5539).

References

Bashkin S and Stoner J O Jr 1975 *Atomic Energy Levels and Grotrian Diagrams I* (Amsterdam: North-Holland)
Böwering N, Döhring T, Gärner U and Heinzmann U 1991 *Laser Particle Beams* **9** 593–601
Dietz E, Braun W, Bradshaw A M and Johnson R L 1985 *Nucl. Instrum. Methods* A **239** 359–66
Fawcett B C 1984 *J. Opt. Soc. Am.* B **1** 195–217
Fawcett B C and Hayes R W 1975 *J. Opt. Soc. Am.* **65** 623–7
Hinze J and Stiehler J 1992 unpublished
Kaufmann V, Sugar J and Rowan W L 1989 *J. Opt. Soc. Am.* B **6** 142–5
Krumrey M, Tegeler E, Barth J, Krisch M, Schäfers F and Wolf R 1988 *Appl. Opt.* **27** 4336–41
Martinson I 1989 *Rep. Prog. Phys.* **52** 157–225
Moore C E 1971 *Atomic Energy Levels* vol I, II (Washington, DC: US Govt Printing Office)
O'Sullivan G 1992 *Comment. At. Mol. Phys.* **28** 143–78
Shirai T, Funatake Y, Mori K, Sugar J, Wiese W L and Nakai Y 1990 *J. Phys. Chem. Ref. Data* **19** 127–275
Shirai T, Nakagaki T, Nakai Y, Sugar J, Ishi K and Mori K 1991 *J. Phys. Chem. Ref. Data* **20** 1–81